

# Hybrid Piezoelectric-Triboelectric Biomechanical Harvesting System for Wearable Applications

Pratibha Verma, Sourav Naval, Dhiman Mallick, *Member, IEEE*, Ankesh Jain, *Senior Member, IEEE*

**Abstract**—This work presents the design and architecture of a miniaturized hybrid energy harvesting system involving Piezoelectric (PEG) and Triboelectric (TEG) generators for scavenging biomechanical energy from various body movements. A combination of PEG and TEG is integrated within a single-substrate device topology that offers the prime advantages of high-output, low-cost, flexible, and compact device design. A novel circuit architecture involving active rectifiers and switched capacitors is proposed to combine these generators' outputs. The interface and power management circuit (PMC) is designed using 180 nm CMOS process. The device simulations and circuit analysis for the proposed hybrid harvesting system indicate an enhanced electrical output compared to standalone harvesters. The simulation results are backed by rigorous experimental investigations on a system prototype consisting of a low-cost TEG device assembled using off-the-shelf materials and a PMC realized using discrete components on a printed circuit board (PCB). The hybrid output of the system charges a  $1\mu F$  load capacitor to  $3.1V$  in  $20s$ . The proposed system generates a peak output power of  $2.76\mu W$  across a  $20M\Omega$  resistive load under a mechanical pressure of  $50kPa$  at  $5Hz$  frequency, which demonstrates its suitability to harness energy from any biomechanical activity to power a diverse range of wearable devices.

**Index Terms**—hybrid generators, power management, interface circuits, biomechanical harvesting, piezoelectric, triboelectric

## I. INTRODUCTION

THE proliferation of low-power wireless devices and self-powered sensor nodes [1], [2] has surged exponentially in the last decade due to the rapid advancements in Internet of Things (IoT) applications. These IoT nodes perform processing and networking functions and thereby have a finite amount of power consumption. A vast majority of these sensing devices are associated with the human body in the form of wearables or in the ambience of the human body. It, therefore, seems logical to harness the energy [3] from biomechanical activities to power such devices. This has ushered the research towards biomechanical harvesting [4] in the past decade. Piezoelectric and Triboelectric mechanisms are widely used for scavenging the low-frequency mechanical excitations associated with human motion or limb movement. They offer the merits of flexibility, low cost, a wide choice of materials, compact topology, and easy integration with the human body.

Many works have been reported based on either Triboelectric and Piezoelectric mechanisms targeting biomechanical applications. However, there is a limit to the amount of mechanical energy captured and transformed by a single harvesting mechanism alone. Therefore, multiple energy harvesting mechanisms are employed together to boost the

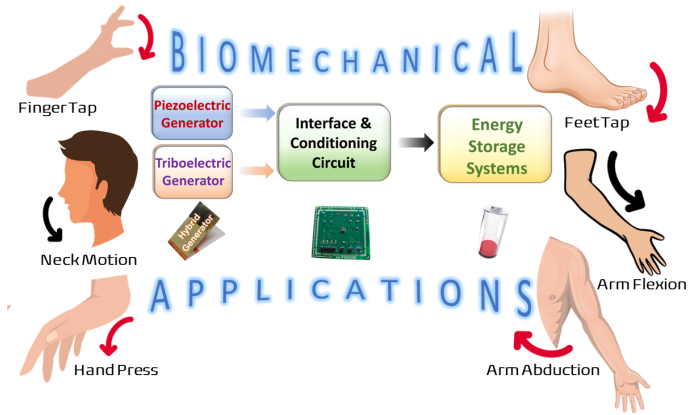


Fig. 1. Overview of this work: Outline of proposed hybrid energy harvesting system and corresponding applications in harvesting biomechanical energy from various body movements

electrical output of the device. Even though the Piezoelectric (PEG) [5] and Triboelectric (TEG) [6] generators have different operation mechanisms [7], they are quite similar in their topology. This fact has been exploited by researchers in designing hybrid energy generators (HEG) [8]–[10] involving both these mechanisms. The transducers convert mechanical vibrations to alternating current that needs to be interfaced and conditioned [11] before it can be used to charge the load or energy storage unit. Researchers have extensively studied the power management circuit (PMC) design strategies pertaining to individual harvesting mechanisms. However, none of the works report the design of a unified PMC unit for hybrid piezoelectric-triboelectric devices.

In this work, we aim to provide a system-level solution to the above-mentioned challenges, as shown in Fig. 1 for a HEG comprising of PEG and TEG. The proposed system includes a single-substrate, flexible device topology with hybrid transduction for enhanced energy conversion efficiency and a suitable power management circuit. The compact and single substrate design makes it flexible yet robust, which is ideal for integrating at different body joints (Fig. 1(b)) for harvesting and sensing applications. The AC outputs of both these generators are applied to a proposed conditioning circuit that rectifies and combines the output of both generators. The boosted hybrid DC output is used to supply power or charge the loads. This article focuses individually on both the device and the circuit design aspects. The device topology and simulations are initially presented, followed by an elaborate study of the PMC.

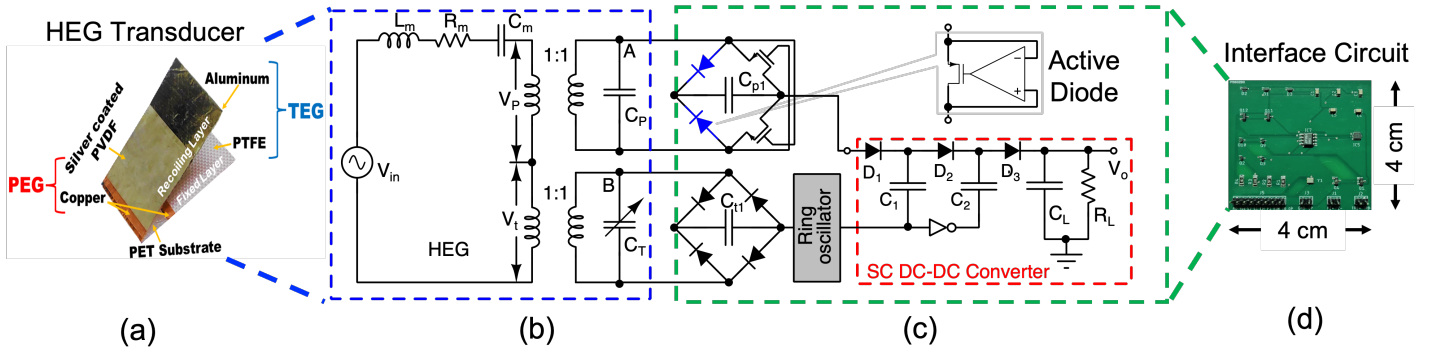


Fig. 2. (a) Photograph of the fabricated prototype of proposed HEG system. (b) EM equivalent model of the HEG device (c) Schematic of proposed power management circuit. (d) Fabricated Power Management Circuit (PMC) in 2-layer PCB.

## II. PROPOSED SYSTEM DESIGN

### A. Device Topology and Working Mechanism

The 3-D structural topology of the designed HEG device is illustrated in Fig. 2(a). It consists of a single polyethylene terephthalate (PET) substrate ( $6 \times 2 \times 0.017 \text{ cm}^3$ ) bent in a V-shape. It has fixed and recoiling layers with a joint at the vertex. TEG and PEG units are integrated within the single topology to improve the efficiency and functionality of the device significantly. The PEG consists of a piezoelectric material polyvinylidene difluoride (PVDF) ( $2 \times 2 \times 0.002 \text{ cm}^3$ ) sandwiched between a coated silver electrode at the top and a copper electrode beneath it. The triboelectric layers (aluminum (Al) and polytetrafluoroethylene (PTFE)) ( $2.5 \times 2 \times 0.002 \text{ cm}^3$ ) are placed at the tip of the recoiling and fixed layers, respectively. The working mechanism of the proposed device can be summarized as follows: When the tip of the recoiling layer is bent, stress is generated within the recoiling layer, and the PEG generates current. The operation of TEG is based on contact electrification and electrostatic induction. When two materials with different electron affinities come into contact, an equal and opposite amount of charge builds up on the surfaces of both materials because of the transport of electrons across different work functions. As the Al layer approaches the PTFE film applied on the base of the fixed layer. This induces the flow of electrons between the TEG electrodes until the two surfaces contact within the same plane and surface charges are neutralized. Once the force is released, the recoiling layer begins to restore to its original position due to its inherent restoring force. As the two surfaces separate, electrons flow back between the TEG electrodes but in the opposite direction. Similarly, in the PEG, as the recoiling layer retracts to its original position, a reverse current flow occurs between the electrodes. Both generators, therefore, generate a cyclic flow of electrons during a single contact-separation cycle, which constitutes an AC output.

### B. Circuit Topology and Operation

Fig. 2(c) illustrates the schematic of the proposed PMC for HEG. The two energy harvesters are represented using their corresponding equivalent electromechanical (EM) model as shown in Fig.2(b) and excites the PMC shown in Fig.

2(c). The EM model for both generators is identical except for their electrical capacitance. The PEG has a fixed capacitor  $C_P$ , which arises from the separation of positive and negative charges across the piezoelectric layer. It remains constant due to the fixed thickness of the piezoelectric layer. For an elastic substrate layer ( $m, k, c$ ), the electrical output of the PEG under an applied force  $F$  can be represented using (1) and (2):

$$m\ddot{x} + c\dot{x} + kx + K_o V_p = F \quad (1)$$

$$C_P \dot{V}_p + \frac{V_p}{R} = K_o \dot{x} \quad (2)$$

where  $K_o$  is the electrically induced damping co-efficient of the PEG, and  $x$  is the resulting displacement of the elastic layer. The output capacitance of TEG is a variable capacitor  $C_T$  due to the periodic contact and separation between the TEG layers caused by vibrations. The varying electric potential ( $V_t$ ) between the layers coupled with varying capacitance causes a charge flow  $q$  between the electrodes, which is mathematically represented below using (3):

$$R \frac{dq}{dt} = \frac{-q}{C_T} + V_t \quad (3)$$

The working of PMC is as follows, The mechanical vibration stimulates a current in HEG which is comprised of TEG and PEG and charges its output capacitor  $C_P$  and  $C_T$  respectively. When proposed PMC is interfaced with HEG then these currents are conditioned using separate bridge rectifier circuits and rectified currents charge output capacitor of each bridge rectifier  $C_{p1}$  and  $C_{t1}$  respectively. However, charging of  $C_{p1}$  (or  $C_{t1}$ ) begins only when the output across  $C_P$  (or  $C_T$ ) is higher than  $2V_D$  where  $V_D$  is the cut in voltage of diode used in bridge rectifier circuit. This creates a problem for PEG output as its swing is rather small and hence the diode remain in forward bias only for a short duration and thus harvesting a very small output. Hence in our proposed PMC we have rather used an active bridge rectifier for PEG path. The active bridge rectifier is realized using a negative voltage converter (NVC) [12]. Unlike a conventional bridge rectifier, it does not use any physical diode. Instead, it involves active diodes and cross-connected NMOS transistors. The active diode [13] realized in this circuit involves a PMOS transistor whose gate voltage is driven by a comparator. The comparator compares the voltage at the drain (anode) and source (cathode) terminals

of the transistor and switches the PMOS on only when the anode voltage exceeds that of the cathode. This switching behaviour is similar to that of a diode; however, it can offer a small  $V_{DS}$  voltage drop compared to the significantly high threshold values of the diodes. This solves the issue of forward voltage drop and finite cut-in voltage associated with diodes as well as diode-connected MOSFETs, reduces power loss, and enhances the DC rectified voltage of PEG. However, this active bridge circuitry has a startup issue. This is not a problem in our proposed PMC as the TEG output is still using the conventional bridge rectifier which is completely passive and works during startup to build up the non zero  $V_o$  which can then activate active bridge rectifier.

The rectified output of the PEG and TEG needs to be combined into a single hybrid output to power the output load. A simple strategy is adopted here to combine the outputs of these generators using a switched capacitor circuit architecture. The DC-DC converter is designed using switched capacitor configuration to eliminate the use of bulky inductors within the circuit and make the circuit compact for wearable applications. This SC DC-DC converter is a hybrid of switched capacitor architecture and Dickson charge pump architecture. The use of an inherent Dickson charge pump boosts the output voltage. The implemented converter topology involves three diodes  $D_1 - D_3$ , two intermediate capacitors  $C_1, C_2$ . The TEG output drives a ring oscillator whose output is fed to the bottom terminal of each of these capacitors in an anti-phase manner. The anti-phase output is created by applying an inverter between the terminals of the capacitors. The voltage at the bottom of the capacitors toggles between low (0) and high ( $V_{DD}$ ) states periodically at a rate of 200Hz. Initially, When the switch oscillator output is low, the PEG output charges the capacitor  $C_1$ . Once the oscillator turns high, the voltage across the junction  $D_1 - C_1 - D_2$  is clamped by a voltage  $V_{DD}$ , and the voltage across the junction becomes  $V_{piezo} + V_{DD} - V_d$ . The boosted voltage now passes through the diode  $D_2$ , sustains a voltage drop  $V_d$  and charges the capacitor  $C_2$  to voltage  $V_{piezo} + V_{DD} - 2V_d$ . Finally, as oscillator output goes low again, the voltage along the output junction  $D_2 - C_2 - D_3$  is boosted by  $V_{DD}$  again, which charges the parallel combination of load capacitor and resistor through diode  $D_3$ . The net output voltage at the load is expressed using (4)

$$V_{out} = V_{piezo} + 2V_{DD} - 3V_d \quad (4)$$

For an  $n$ -stage switched capacitor circuit with  $n$  intermediate capacitors, the resulting output  $V_{out,n}$  can be expressed as a function of the rectified PEG output  $V_{piezo}$ , rectified TEG output  $V_{tribo}$  and the diode forward voltage drop  $V_d$  using (5):

$$V_{out,n} = V_{piezo} + nV_{tribo} - (n+1)V_d \quad (5)$$

### III. EXPERIMENTAL RESULTS AND DISCUSSION

#### A. Device Characterization

The proposed device model is created, and a Finite Element Method (FEM) study is performed on COMSOL Multiphysics. The stress profile developed in the device under a compressive

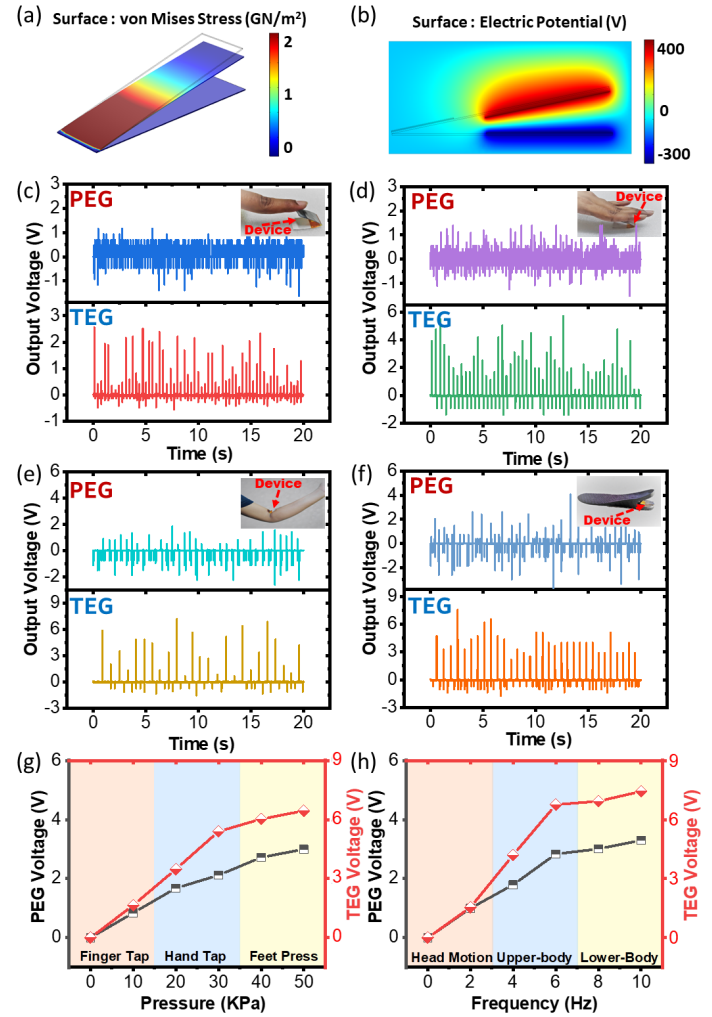


Fig. 3. Device Characterization: (a) Stress profile under compressive load (b) Surface Electrostatic Potential due to surface charges. Experimental Results: Time-domain response of PEG and TEG for device applications during (c) finger-tapping (d) hand-tapping (e) elbow bending (f) as an in-sole device. Variation of device output under varying mechanical (g) pressure (at 5 Hz) (h) frequency (at 50 kPa).

force applied on the tip of the recoiling layer is illustrated in Fig. 3(a). Since maximum stress is developed near the device joint, the piezoelectric layer is applied in that region to extract maximum energy from the generated stress. The surface electric potential study demonstrates the development of positive and negative potentials around the Al and PTFE layers, respectively. The time-domain response of PEG and TEG under different biomechanical stimuli of finger tapping, hand tapping, elbow bending, and as an in-sole device is presented in Fig. 3(c)-(f), respectively. A significant PEG and TEG voltage amplitude generated in all the instances warrants the performance of the proposed device as an efficient biomechanical harvester. The device performance is also characterized by varying pressure and frequency of the applied mechanical stimuli. The range of mechanical inputs is chosen based on the common range of biomechanical stimulus [14]. Most body movements occur at a low frequency (0-10 Hz) and apply pressures between a few to tens of KPa. The



TABLE I  
CIRCUIT COMPONENTS

COMPONENT	MANUFACTURER	MODEL
P-channel MOSFET	On Semi	NTR020PLT1G
N-channel MOSFET	On Semi	NTA7002NT1G
Diode	On Semi	MMDL6050T1G
Comparator	Analog Devices Inc.	LTC1441CS8#PBF
Inverter	Nexperia USA Inc.	74LV04BQ.115
Capacitor	YAGEO	CC0805JKX7R9BB105
Resistor	Bourns Inc.	CR1206-JW-102ELF
Capacitor	Wrth Elektronik	885012206059
Inverter	Texas Instruments	SN74AUP3G14DCUR

TEG and PEG outputs initially show a linear correlation with the applied pressure and frequency, which gradually saturates at higher values, as shown in Fig. 3(g)-(h). An increase in pressure causes increased strain in the recoiling layer and enhances the effective contact area between the recoiling and fixed layer surfaces. These factors contribute to enhanced PEG and TEG outputs, respectively. Once the effective strain and contact area are maximized, the outputs of both generators begin to saturate. Similarly, an increase in frequency increases the velocity of vibration of the recoiling layer until it gradually reaches its saturation velocity. This causes an initial rise in the electron flow rate between the electrodes, which eventually settles at higher frequencies.

### B. PMC Characterization

The system-level functioning of the hybrid piezoelectric-triboelectric system is demonstrated by incorporating the miniaturized hybrid generator with the PMC shown in Fig.4. Its size is 4cm x 4cm which can be further miniaturized as the current PCB has components sparsely placed. The proposed interface PMC is a completely battery-less, self-powered circuit designed to interface, condition, and utilize the output power generated by the transducer for powering IoT applications. The PMC is fabricated on a 2-layer PCB (Fig. 2c) using the components enlisted in Table 1.

The interface circuit is further designed and simulated using 180nm CMOS process. The performance of the proposed

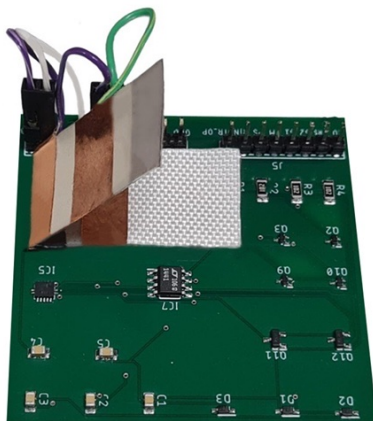


Fig. 4. Prototype of hybrid energy harvester along with power management circuitry

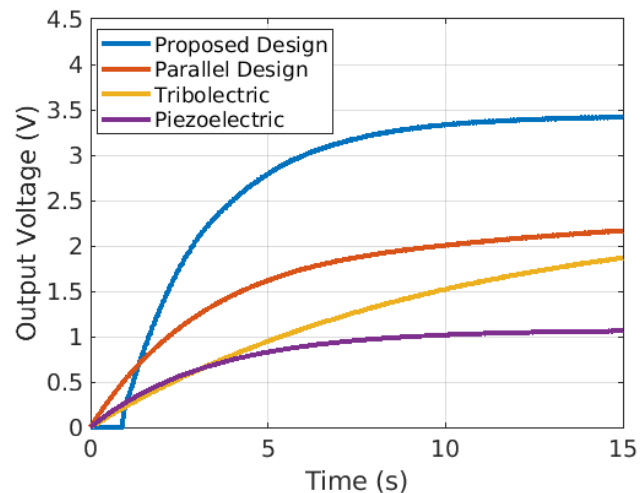


Fig. 5. Simulation results showing improvement in output voltage using the proposed hybrid circuit architecture

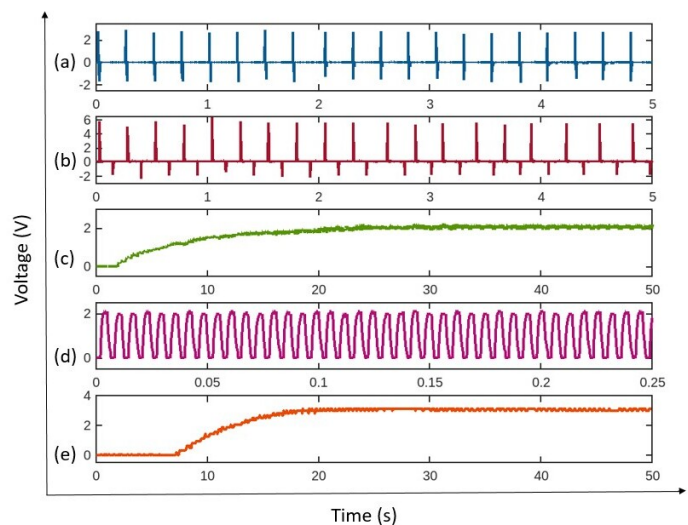


Fig. 6. PMC Characterization: Time domain response of (a) PEG Output (b) TEG Output (c) Rectified TEG Output ( $V_{DD}$ ) (d) Oscillator Output (e) HEG Output

hybrid circuit is compared to that of a conventional bridge rectifier. The output is observed across a  $1\mu\text{F}$  load capacitor and  $10\text{M}\Omega$  load resistance. The charging performance is shown in Fig.5 for the cases in which the load is charged using only TEG, only PEG, parallel rectified outputs of TEG and PEG, and the hybrid output from the proposed circuit topology. Applying the rectified outputs of TEG and PEG in parallel is the most widely adopted strategy [15]–[19] to generate hybrid TEG-PEG output. It is evident that the output voltage is relatively high in the case of hybrid topology depicting the successful combination of EH outputs and it is the most effective method for hybridizing the outputs of these generators.

The HEG is subjected to a mechanical pressure of 50 kPa at a 5 Hz frequency. The AC outputs of the generators are shown in Fig. 6(a, b). Initially, the generated rectified voltage of the

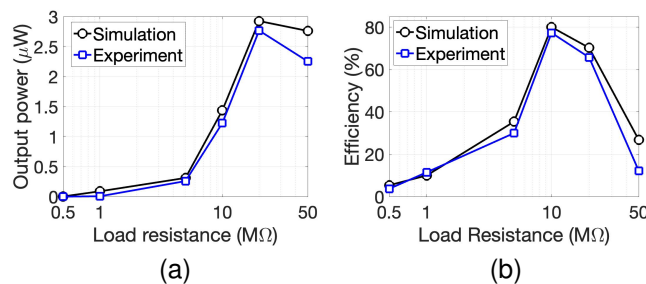


Fig. 7. Experimental results showing (a) Variation of output power (b) Variation of PMC efficiency with load resistance

TEG is drawn by the storage capacitor ( $0.5\mu F$ ), which charges to a value  $V_{DD}$  as shown in Fig. 6(c). When the  $V_{DD}$  voltage exceeds a threshold voltage of 1 V, it acts as a supply source to power the entire circuit. The active diodes and oscillator Fig. 6(d) are powered up, and the load capacitor ( $1\mu F$ ) begins to charge, and it saturates at a constant voltage of 3.1 V after 20 s (Fig. 6(e)).

The circuit performance is then evaluated for different load resistances. The output power is plotted with varying load in Fig. 7(a). The peak output power is  $2.76\mu W$  across a  $20 M\Omega$  resistive load. The output power was computed based on the dc output voltage, while the power drawn from the input of each harvester is estimated by the formula [20]. The Fig.7(b) shows the efficiency of the proposed interface circuit for varying load resistances. The conversion efficiency of the proposed PMC is calculated by the equation,  $\eta = \frac{P_{out}}{P_{TEG} + P_{PEG}}$ , where  $P_{out}$  is hybrid DC output power,  $P_{TEG}$  and  $P_{PEG}$  are the outputs of the two harvesters. The circuit achieves a peak efficiency of 77.33% at an external load of  $10 M\Omega$ .

#### IV. CONCLUSION

In this work, the design and analysis of a biomechanical harvesting system consisting of a hybrid piezoelectric-triboelectric generator and a suitable interface power management circuit (PMC) are presented. The fabrication of the entire device on a single flexible substrate and in a V-shape enables easy integration at human joints and increases the robustness and longevity of the device. The piezoelectric and triboelectric outputs are interfaced using a novel proposed circuit architecture involving rectifiers and switched capacitor-based DC-DC converters. The implemented circuit replaces the conventional diodes with active diodes in bridge rectifier of PEG, thereby reducing power consumption and increasing efficiency. The interface circuit provides a peak efficiency of 77.33% at an external load of  $1 M\Omega$ . The harvesting system charges a  $1\mu F$  load capacitor to 3.1 V in 20 s.

#### ACKNOWLEDGEMENT

The authors would like to thank I-Hub Foundation for Cobotics, Technology Innovation Hub, IIT Delhi, India (Grant Number: RP04218G) for financially supporting this work.

#### REFERENCES

- [1] S. Naval, P. Verma, A. Jain, and D. Mallick, "Hybrid vector and pressure sensor for fingertip dynamics sensing using dc-triboelectric/ac-piezoelectric mechanisms," *Sensors and Actuators A: Physical*, vol. 355, p. 114330, 2023.
- [2] P. Verma, S. Naval, D. Mukherjee, D. Mallick, and A. Jain, "System architecture for conditioning the asymmetric and high crest output of triboelectric generators," *IEEE Sensors Letters*, vol. 7, no. 10, pp. 1–4, 2023.
- [3] D. Mallick, S. Naval, and N. T. Beigh, "MEMS-Based Energy Harvesting Devices: Overview of Recent Progress," in *MEMS Applications in Electronics and Engineering*. AIP Publishing LLC, 2023.
- [4] S. Naval, N. T. Beigh, D. Mukherjee, A. Jain, and D. Mallick, "Flexible v-shaped piezoelectric-triboelectric device for biomechanical energy harvesting and sensing," *Journal of Physics D: Applied Physics*, vol. 55, no. 36, p. 365501, jun 2022.
- [5] N. Sezer and M. Ko, "A comprehensive review on the state-of-the-art of piezoelectric energy harvesting," *Nano Energy*, vol. 80, p. 105567, 2021.
- [6] S. Naval, A. Jain, and D. Mallick, "Direct current triboelectric nanogenerators: a review," *Journal of Micromechanics and Microengineering*, vol. 33, no. 1, p. 013001, dec 2022.
- [7] S. Naval, N. T. Beigh, A. Jain, and D. Mallick, "Bandwidth tunable vibration energy harvester based on hybrid triboelectric-piezoelectric array," *Engineering Research Express*, vol. 4, no. 4, p. 045022, nov 2022.
- [8] J. Sharma, P. Verma, D. Mallick, and A. Jain, "Electrical energy injection using hybrid sece for high performance nonlinear mechanical energy harvesting," in *2021 IEEE International Midwest Symposium on Circuits and Systems (MWSCAS)*, 2021, pp. 80–83.
- [9] S. Chamanian, B. ifci, H. Uluhan, A. Muhtarolu, and H. Klah, "Power-efficient hybrid energy harvesting system for harnessing ambient vibrations," *IEEE Transactions on Circuits and Systems I: Regular Papers*, vol. 66, no. 7, pp. 2784–2793, 2019.
- [10] H. Uluhan, S. Chamanian, W. M. P. R. Pathirana, . Zorlu, A. Muhtarolu, and H. Klah, "Triple hybrid energy harvesting interface electronics," *Journal of Physics: Conference Series*, vol. 773, no. 1, p. 012027, nov 2016.
- [11] S. Naval, P. Verma, N. T. Beigh, D. Mukherjee, A. Jain, and D. Mallick, "Flexible dc triboelectric generator with associated conditioning circuit," in *2022 21st International Conference on Micro and Nanotechnology for Power Generation and Energy Conversion Applications (PowerMEMS)*, 2022, pp. 30–33.
- [12] G. Singh, S. Pal, and S. Kundu, "Robust vibration invariant sshi rectifier circuit for piezoelectric device," *Analog Integr. Circuits Signal Process.*, vol. 111, no. 1, p. 5770, apr 2022.
- [13] M. Lipski, Y. Li, M. Misra, and S. Gregori, "A low forward bias active diode circuit for electrostatic energy harvesters," in *2018 IEEE International Symposium on Circuits and Systems (ISCAS)*, 2018, pp. 1–5.
- [14] D. Qiao, G. K. Pang, M. M. Kit, and D. C. Lam, "A new pcb-based low-cost accelerometer for human motion sensing," in *2008 IEEE International Conference on Automation and Logistics*, 2008, pp. 56–60.
- [15] W. Wang, J. Zhang, Y. Zhang, F. Chen, H. Wang, M. Wu, H. Li, Q. Zhu, H. Zheng, and R. Zhang, "Remarkably enhanced hybrid piezo/triboelectric nanogenerator via rational modulation of piezoelectric and dielectric properties for self-powered electronics," *Applied Physics Letters*, vol. 116, no. 2, p. 023901, 01 2020.
- [16] X. Chen, M. Han, H. Chen, X. Cheng, Y. Song, Z. Su, Y. Jiang, and H.-X. Zhang, "Wavy-shaped hybrid piezoelectric and triboelectric nanogenerator based on p(vdf-trfe) nanofibers," *Nanoscale*, vol. 9, 01 2016.
- [17] A. Mahmud, A. A. Khan, S. Islam, P. Voss, and D. Ban, "Integration of organic/inorganic nanostructured materials in a hybrid nanogenerator enables efficacious energy harvesting via mutual performance enhancement," *Nano Energy*, vol. 58, pp. 112–120, 2019.
- [18] M. Han, X.-S. Zhang, B. Meng, W. Liu, W. Tang, X. Sun, W. Wang, and H.-X. Zhang, "r-shape hybrid nanogenerator with enhanced piezoelectricity," *ACS nano*, vol. 7, 09 2013.
- [19] S. Qin, Q. Zhang, X. Yang, M. Liu, Q. Sun, and Z. L. Wang, "Hybrid piezo/triboelectric-driven self-charging electrochromic supercapacitor power package," *Advanced Energy Materials*, vol. 8, no. 23, p. 1800069, 2018.
- [20] A. Romani, M. Filippi, M. Dini, and M. Tartagni, "A sub- a stand-by current synchronous electric charge extractor for piezoelectric energy harvesting," *J. Emerg. Technol. Comput. Syst.*, vol. 12, no. 1, aug 2015.